Calculation of single-beam two-photon absorption transition rate of rare-earth ions using effective operator and diagrammatic representation

Chang-Kui Duan[a,b,*], Michael F. Reid[b], Gang Ruan[a], Hui-Ning Dong[a]

[a] *Institute of Applied Physics and College of Electronic Engineering, Chongqing University of Posts and Telecommunications, Chongqing 400065, China*
[b] *Department of Physics and Astronomy, University of Canterbury, Christchurch, New Zealand*

Abstract

Effective operators needed in single-beam two-photon transition calculations have been represented with modified Goldstone diagrams similar to the type suggested by Duan et al. [C.-K. Duan, G. Ruan, M.F. Reid, J. Chem. Phys. 121 (2004) 5071]. The rules to evaluate these diagrams are different from those for effective Hamiltonian and one-photon transition operators. It is verified that the perturbation terms considered contain only connected diagrams and the evaluation rules are simplified and given explicitly.
© 2005 Elsevier B.V. All rights reserved.

1. Introduction

Two-photon laser spectroscopy has been used as an important complementary technique in studying optical materials containing lanthanide ions. A recent short review can be found in [1]. Two-photon excitation in a conventional microscope studying biological samples provides great advantages, including low photo-damage and depth discrimination, reduced photobleaching, good separation of the excitation light from the fluorescence emission [2]. Two-photon lasers could give rise to entangled twin beams which offer potential for novel future applications [3]. A theoretical challenge in the field of two-photon spectroscopy is prediction of two-photon transition rates [1,4,5].

Our work focuses on the calculation of single-beam two-photon absorption rates, in particular for optical materials with lanthanides ions. In a former paper [6], we have presented the effective operator method and given a perturbation expansion. In this paper we show that the perturbation expansion can be represented with a kind of diagrams, which

can be calculated using one and two-particle matrix elements of interactions and single-particle energies. In Section 2, we show how to derive the diagrams from the perturbation expansion; Section 3 presents those diagrams with only valence internal lines and unusual energy denominators; In Section 4 we show the cancellation of disconnected diagrams.

2. Construction of diagrams from perturbation expansions

The calculation of two-photon transition rates has been reduced to the calculation of an effective transition operator [6]. The square modulus of the matrix element of the effective operator between two eigenstates of the effective Hamiltonian (usually approximated with semi-classical phenomenological Hamiltonian) is the two-photon transition line strength that can be compared to measurements. In [6], the effective operator is partitioned into two terms. The first term is calculated with "direct method" [5,6], and the second term is calculated using many-body perturbation theory. It has been shown [5] that this method contains more general contribu-

* Corresponding author. Tel.: +86 23 62460554; fax: +86 23 62460554.
E-mail address: duanck@cqupt.edu.cn (C.-K. Duan).

tions than previous methods. Here, we start from that expansion for the second term and consider the usual case where the model space P_{I0} and P_{F0} are the same complete model space, denoted as P_0. By "complete model space" we mean that the model space contains all the bases that can be formed by distributing the valence electrons among the valence single particle states [7,8]. Denoting the space orthogonal to P_0 by Q_0, the perturbative expansion is simplified into the following form

$$\langle f|T^2_{\text{eff},0}|i\rangle = \frac{\langle f|O|k\rangle\langle k|O|i\rangle}{(E_{f0} + E_{i0})/2 - E_{k0}} \quad (1)$$

$$\langle f|T^2_{\text{eff},1}|i\rangle = \frac{\langle f|V|k_1\rangle\langle k_1|O|k_2\rangle\langle k_2|O|i\rangle}{(E_{f0} - E_{k_10})[((E_{f0} + E_{i0})/2) - E_{k_20}]} \quad (2)$$

$$+ \frac{\langle f|O|k_1\rangle\langle k_1|O|k_2\rangle\langle k_2|V|i\rangle}{[((E_{f0} + E_{i0})/2) - E_{k_10}](E_{i0} - E_{k_20})} \quad (3)$$

$$+ \frac{\langle f|O|l\rangle\langle l|V|k\rangle\langle k|O|i\rangle}{[((E_{f0} + E_{i0})/2) - E_{k0}](E_{k0} - E_{l0})} \quad (4)$$

$$+ \frac{\langle f|O|k\rangle\langle k|V|l\rangle\langle l|O|i\rangle}{(E_{k0} - E_{l0})[((E_{f0} + E_{i0})/2) - E_{k0}]} \quad (5)$$

$$+ \frac{\langle f|O|k_1\rangle\langle k_1|V|k_2\rangle\langle k_2|O|i\rangle}{[((E_{f0} + E_{i0})/2) - E_{k_10}][((E_{f0} + E_{i0})/2) - E_{k_20}]} \quad (6)$$

$$- \frac{1}{2} \frac{\langle f|V|l\rangle\langle l|O|k\rangle\langle k|O|i\rangle}{[((E_{f0} + E_{i0})/2) - E_{k0}][((E_{l0} + E_{i0})/2) - E_{k0}]} \quad (7)$$

$$- \frac{1}{2} \frac{\langle f|O|k\rangle\langle k|O|l\rangle\langle l|V|i\rangle}{[((E_{f0} + E_{l0})/2) - E_{k0}][((E_{f0} + E_{i0})/2) - E_{k0}]}, \quad (8)$$

where $T^2_{\text{eff},i}$ is the part of effective operator zeroth ($i = 0$) and first order ($i = 1$) in V, k, k_1 and k_2 sum over many-particle orthonormal eigenstates of H_0 in Q_0 and l sums over eigenstates of H_0 in P_0. f and i are orthonormal eigenstates of H_0 in P_0.

The perturbation V contains both a one-body operator, denoted as V_1 and a two-body operator, denoted as V_2. Usually the operator O is one-body operator. Using algebraic representation and corresponding diagrammatic representation given in [9], Eqs. (1) and (4), O, V_1 and V_2 can be represented by 4, 4 and 9 diagrams, respectively. Compositions of two O's and one V_1 or V_2, as given in Eq. (2)–(8), with all possible contractions and all possible relative positions, result into hundreds of diagrams. This prompts us to adapt the modified diagrams given in [9] to combine the set of diagrams with the same set of vertices, line directions and contractions but different relative position and internal orbit types into one diagram.

2.1. Adapted connected diagrams with vertices V_1 and two O

There are altogether three ingoing and three outgoing lines, with at least two pairs of them contracted to form
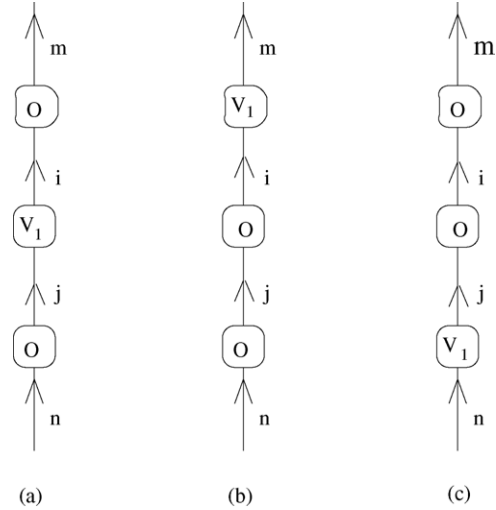

Fig. 1. Modified one-body diagrams first order in V_1 for one-beam two-photon transition moment. Note that: (1) the internal lines can be both particle lines and core lines, and the relative altitudes of two O's and V_1 change accordingly; (2) contributions of (b) and (c) to the effective operator are complex conjugation of each other.

connected diagrams. Therefore the connected diagram can only be zero-body (a constant) or one-body diagrams. A constant will not contribute to any transition, which is neglected throughout of this paper.

There are three modified one-body diagrams as shown in Fig. 1. Similar to the case for effective one-photon transition operators in Fig. 4 of [9], each diagram actually represents contributions from several different terms in Eq. (2)–(8). For example Fig. 1(a), with different internal line types, includes contributions from Eqs. (2), (3) and (6). Note that the energy denominator rules will be slightly different from those for effective one-photon transition operators in [9].

2.2. Adapted connected diagram with vertices V_2 and two O

There are altogether 4 ingoing and 4 outgoing lines for one V_2 and two O. Therefore connected diagrams can be zero-body, one-body and two-body.

There are also three modified one-body diagrams as shown in Fig. 2, and five modified two-body diagrams as shown in Fig. 3, where two diagrams complex conjugate to Fig. 3(b) and (c) are not given explicitly.

Similar to connected diagrams in Fig. 1, Fig. 2(a) includes contributions from Eq. (2), (3) and (6). These contributions form altogether 6 different normal diagrams. Note that the energy denominator rules for contributions from different terms are slightly different.

2.3. Rules to evaluate these diagrams

Remembering that each modified diagram actually represents a set of diagrams with different ordering of vertices and different types of internal lines, it is not difficult to obtain the
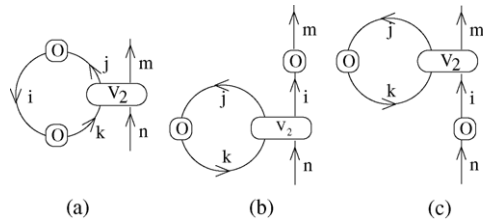
Fig. 2. Modified one-body diagrams first order in V_2 for one-beam two-photon transition moment. Note that: (1) the internal lines can be both particle lines and core lines, and the relative altitudes of two O's and V_1 change accordingly; (2) there are natural constrains over several internal lines forming a close loop, since particle lines go upward and core lines go downward, for example, in (b), $\{j, k\}$ must be one particle line and one hole line; (3) contributions of (b) and (c) to the effective operator are complex conjugation of each other.
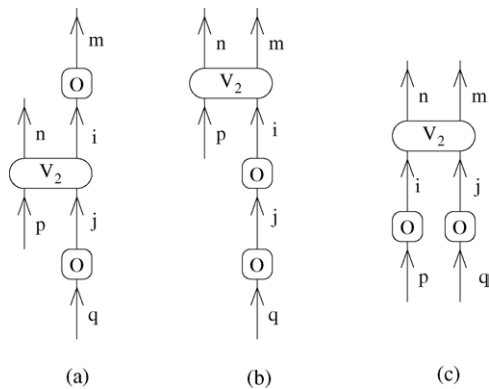

Fig. 3. Modified two-body diagrams first order in V_2 for one-beam two-photon transition moment. Note that: (1) the internal lines can be both particle lines and core lines, and the relative altitudes of two O's and V_1 change accordingly; (2) two diagrams with contributions complex conjugate to these of (b) and (c) are not shown here.

analytic expressions for these diagrams. For each diagram with fixed vertex ordering, the expression can be calculated by the same rules (1)–(7) given in Section 2 [10], except that the rule to calculate energy denominators in rule (6) should be modified as follows: denoting the net outflow energy of a loop enclosing vertices $1, 2, \cdots, i$ as

$$E_{\text{noe}}(1, 2, \cdots, i) = E_{\text{noe}}(1) + E_{\text{noe}}(2) + \cdots + E_{\text{noe}}(i), \quad (9)$$

and supposing the number of O in the loop is i_O ($i_O = 0, 1, 2$) and the number of vertices for the diagram is n, the energy denominator can be written as

$$D = \prod_{i=1}^{n-1} \left(\frac{i_O}{2} E_{\text{noe}}(1, 2, \cdots, n) - E_{\text{noe}}(1, 2, \cdots, i) \right). \quad (10)$$

3. Diagrams with vertex operators acting only on model spaces P_0

Eqs. (4), (5), (7) and (8) give diagrams with some vertices, whose bra states and ket states are in model spaces P_0. As

an example, Eq. (4) have the same operator sequence OVO as that of Eq. (6), but different denominators. They will give diagrams with different evaluation rules, similar to but not exactly the same as those terms in effective Hamiltonian that give folded diagrams [11–13]. Instead of introducing new folded diagrams, we combine these contributions to the diagrams given above. The rules to evaluate these contributions differ from standard rules in an overall factor $-1/2$ for diagrams from Eqs. (7) and (8), and in energy denominators by using rules given in Eqs. (4), (5), (7) and (8).

4. Cancellation of disconnected diagrams

For modified disconnected diagrams with one V vertex and two O vertices, there must be a connected part with only one vertex, which is either V or O.

Case A: V is disconnected from other parts. In this case both the ingoing and the outgoing lines of V are valence lines. Such a diagram includes contributions from Eqs. (6)–(8) with the same matrix elements but different coefficients due to different energy denominators. Suppose the net-outgoing-energies from the first O and the second O vertices are ΔE_1 and ΔE_2, respectively, and that from the V is ΔE_3. The three different coefficients for the three contributions from Eqs. (6)–(8), respectively, are as follows:

$$\frac{1}{[(((\Delta E_1 + \Delta E_3 + \Delta E_2) + 0)/2) - (\Delta E_3 + \Delta E_2)]} \quad (11)$$
$$\times [(((\Delta E_1 + \Delta E_3 + \Delta E_2) + 0)/2) - \Delta E_2]$$

$$+ \left(-\frac{1}{2} \right) \frac{1}{[(((\Delta E_3 + \Delta E_1 + \Delta E_2) + 0)/2) - \Delta E_2]} \quad (12)$$
$$\times [(((\Delta E_1 + \Delta E_2) + 0)/2) - \Delta E_2]$$

$$+ \left(-\frac{1}{2} \right) \frac{1}{[(((\Delta E_1 + \Delta E_2 + \Delta E_3) + 0)/2)}$$
$$- (\Delta E_2 + \Delta E_3)][(((\Delta E_1 + \Delta E_2 + \Delta E_3)$$
$$+ \Delta E_3)/2) - (\Delta E_2 + \Delta E_3)]$$

$$\qquad (13)$$

$$= 0 \qquad (14)$$

Case B: one O is disconnected from other parts. Such a diagram includes contributions from Eqs. (2)–(5). It can be verified in the same way as above that all these contributions cancel.

5. Conclusion

Diagrams for two-photon transitions rates have been constructed and have been shown to be connected. Simplified one-photon diagrams given in J. Chem. Phys. 121 (2004)

5071 have been adapted to two-photon cases. The algebraic expressions suitable for a general two-photon calculation can be given from these diagrams.

Acknowledgment

References

[1] C.-K. Duan, M.F. Reid, G.W. Burdick, Phys. Rev. B 66 (2002) 155108.
[2] M.D. Cahalan, I. Parker, S.H. Wei, M.J. Miller, Nat. Rev. Immunol. 2 (2002) 872.
[3] B.H. Cumpston, S.P. Ananthavel, S. Barlow, D.L. Dyer, J.E. Ehrlich, L.L. Erskine, A.A. Heikal, S.M. Kuebler, I.-Y.S. Lee, D. Mccord-Maughon, et al., Nature 398 (1999) 51.
[4] M.C. Downer, in: W.M. Yen (Ed.), in: Laser Spectroscopy of Solids II, Springer-Verlag, 1989 (Chapter 2).
[5] G.W. Burdick, M.F. Reid, C.-K. Duan, J. Chong, A. Burdick, The puzzle of two-photon rare earth spectra in solids · · · solved?—for dpc'03, New Zealand (2003), Presented at International Conference on Dynamical Processes of Excited States in Solids, Christchurch, New Zealand, 2003.
[6] C.-K. Duan, G. Ruan, M.F. Reid, J. Chem. Phys. 121 (2004) 8183.
[7] C.-K. Duan, M.F. Reid, J. Chem. Phys. 115 (2001) 8279.
[8] I. Lindgren, Phys. Scr. 32 (1974) 611.
[9] C.-K. Duan, G. Ruan, M.F. Reid, J. Chem. Phys. 121 (2004) 5071.
[10] C.-K. Duan, G. Ruan, M.F. Reid, J. Chem. Phys. 121 (2004) 5076.
[11] B.H. Brandow, Rev. Mod. Phys. 39 (1967) 771.
[12] I. Lindgren, Phys. Scr. 32 (1985) 291.
[13] T.T.S. Kuo, E. Osnes, Folded-Diagram Theory of the Effective Interaction in Nuclei, Atoms and Molecules, Vol. 364 of Lecture Notes in Physics, Springer-Verlag, 1990.